JETIR.ORG ISSN: 2349-5162 | ESTD Year : 2014 | Monthly Issue
JOURNAL OF EMERGING TECHNOLOGIES AND INNOVATIVE RESEARCH (JETIR)
An International Scholarly Open Access, Peer-reviewed, Refereed Journal

Industrial Internet of Things IN D2D communication using LiFi technology

1NAME: Dr.B.Nancharaiah,2NAME: Y. ESWAR, 3NAME: K. NAGA MOUNIKA DEVI, 4NAME: V. RAKESH BABU

5NAME: V. VAMSI KRISHNA

Designation of Author1:HOD, Designation of 2Author: B.E, MTech, Designation of Author3: B.E, MTech,
Designation of Author4: B.E, MTech, Designation of Author5: B.E, MTech
Name of Department of :, ELECTRONICS AND COMMUNICATION AND ENGIEERING
[1]Name of organization of : USHA RAMA ENGIEERING COLLAGE , VIJAYAWADA, INDIA

Abstract : Abstract— In the context of the industrial Internet-of-things (IIoT), this study explores the performance evaluation of device-to-device (D2D) communication using light fidelity (LiFi). An extensive analysis of industrial LiFi networks' mobility management is provided. Based on the semi angle at half illuminance of the access point (AP) and D2D transmitting IIoT devices, a coverage model for the D2D communication range is generated. We provide closed-form formulas that use stochastic geometry to calculate the mode selection rate and residence time. These expressions are dependent on velocity, IIoT density, and AP density. According to our research, denser deployment and higher velocity cause the average D2D transition rate to rise and the average D2D residence duration to decrease, or vice versa. We use MATLAB simulations to evaluate the suggested analytical models, providing important information for system-level design. Device-to-device (D2D), LiFi, optical wireless communication, visible light communication, Industrial Internet-of-Things (IIoT), and other concepts are important to understand.

I. INTRODUCTION

There won't be enough radio spectrum accessible for mobile communications in the future due to the constant rise in data transmission [1]. Device-to-device (D2D) communication, which enables direct connection between any two adjacent D2D user equipment (DUE) to increase system capacity and spectral efficiency, is a viable option for making effective use of the spectrum [2]. Several D2D pairs can share the same radio frequency (RF) band in order to increase system capacity [3]. Furthermore, other bands, such Bluetooth or LiFi, that are not part of the RF licensed channels, can be utilized [4]. Utilizing visible light communications (VLC) at frequency ranges between 400 and 790 THz is another alluring choice. Because of this, VLC is appropriate for short-distance communication, such as inside [5]. Numerous research (e.g., [6]-[7]) highlight the advantages of D2D communication utilising solely VLC bands. However, because the VLC connection is very sensitive to variations in the irradiance of the transmitter (DUEt) and the incidence angles of the receiver (DUEr), it may experience abrupt decreases in channel quality. For this reason, VLC connections must always have the ability to revert to RF. A preliminary investigation of the use of VLC and RF together for D2D communication is provided in [1]. Next, by choosing an RF or VLC communication band for each pair, an iterative two-phase heuristic approach is presented in [8] to minimise the outage and maximise the sum capacity of D2D pairings. But [8]'s solution is predicated on the idea that channel gains among all DUEs in VLC and RF are identified. Furthermore, the iterative process used in [8]'s band selection is unsuitable for dynamic settings when a quick band selection is necessary. We formulate the band selection issue as a supervised binary classification problem that aims to pick either RF or VLC for each D2D pair, avoiding the necessity for full channel information. To minimize outages and maximize average energy efficiency of D2D communication, we assume just the received power and received total interference at each DUEr in RF and VLC. This band selection challenge is resolved by using a deep neural network (DNN).

I. LITERATURE SURVEY

Mobility management has been studied extensively in both RF networks and hybrid RF-LiFi configurations The majority of prior research has focused on hybrid RF-LiFi network vertical handover strategies. In the case of hybrid RF-LiFi networks, for example, [10] looks into the possibility of vertical handovers for users who encounter unpredictable rotations. Furthermore, in order to improve vertical handovers, [11] suggests a Markov decision method, while [12] presents a
vertical handover scheme based on predicted criteria including access latency, data size, and interruption length. In order to overcome line-of-sight (LoS) blocking concerns, Chowdhury and Katz [13] evaluate the performance of hybrid RF-LiFi hot-spot networks in mobile settings and provide fuzzy logic-based vertical handover algorithms. Because of the difference in air interfaces, vertical handovers usually need longer Systems often have less capacity than LiFi, and too many RF users might drastically limit throughput. Thus, in vertical handover schemes, Much emphasis has been paid to resource allocation, optimization, and dynamic load balancing. [8].There is potential for a variety of scenarios and applications when RF and VLC are combined for D2D communication. This includes communication between gadgets of all kinds, from traditional cell phones [27] to Internet of Things

gadgets and home appliances [28]. Such scenarios can be found in industrial settings or healthcare institutions [28], where people interact with machines and other technologies. Users in a room might converse with household appliances, share presentations, or trade data. Systems often have less capacity than Lifi, and too many RF users might drastically limit throughput. Thus, in vertical handover schemes, Such scenarios can be found in industrial settings or healthcare institutions [28], where people interact with machines and other technologies. Users in a room might converse with household appliances, share presentations, or trade data. Outdoor settings for smart city projects [28] or vehicle-to-vehicle communication [27, 29] present another interesting use. In this scenario, D2D is used for direct vehicle communication. across VLC bands, enabling the transfer of large amounts of data from many sensors. For example, let's say a truck streams footage to automobiles behind it whose vision is blocked by the truck's front camera. Moreover, unmanned aerial vehicle (UAV) situations find use for D2D communication over VLC [30, 31]. Through D2D communication, UAVs may operate as both users and base stations. Nevertheless, they confront similar issues as VLC-based D2D communication due to their dynamic nature and constant location changes. The mobility management of D2D communication combining RF and VLC bands is the main topic of this article.

II. PROPOSED METHOD

The following is a summary of the project's principal contributions:

- Using the semi-angle of the access point (AP) and D2D transmitting IIoT devices, we offer an analytical methodology for determining the range of LiFi-mediated device-to-device (D2D) communication for scenarios involving the Industrial Internet of Things (IIoT).
  A closed-form formula that accounts for device velocity, AP density, IIoT density, and the transmitters' semi-angle at half illuminance is used to determine the D2D mode transition rate and D2D mode residence time.
- We do extensive simulations using MATLAB to verify the precision and effectiveness of the analytical model
- The research looks into how different system characteristics, such user speed, affect the efficiency of communication. The analysis's conclusions are essential for the realistic planning and development of industrial LiFi networks.

III. SYSTEM MODEL

The D2D network model that is suited for mobile IIoT devices is presented in this part and forms the basis of our investigation. First, we use the Poisson–Voronoi tessellation in conjunction with a Poisson point process (PPP) model to disperse the IIoT devices and access points (APs) over the network. We then offer some insights into the LiFi channel model that we used in our investigation. We also provide the mobility model created especially for the IIoT devices in the research.

Network Model

In LiFi network research, cells have typically been modelled using square or hexagonal geometries. But it is not feasible to try to use a well-defined deterministic or regular model for device positioning in very thick industrial LiFi networks with A vast number of "statistically random" APs and IIoT devices, such as sensors, drones, robotic arms, and self-driving automobiles. Therefore, it is thought to be more accurate and useful to use stochastic geometry to simulate the distribution of nodes in industrial LiFi networks. Stochastic geometry, often referred to as random spatial models, is based on the idea that because wireless network users are varied and unpredictable, node placements and related properties are essentially random. As such, a thinning procedure is frequently used in real-world situations to duplicate the locations of LiFi APs. Because it depends on user locations and mobility profiles, which both have unpredictable behavior, this thinning process is stochastic.

A large portion of current research is based on computer simulations due to the analytical difficulties of no stochastic models. However, it is acknowledged that in order to comprehend the ways in which various network factors impact network performance, an analytical framework is necessary. The use of stochastic geometry in this study is justified since it provides mathematical tractability and the capacity to predict the performance of real-world LiFi networks. Randomly positioned points with an intensity parameter (λ) in a mathematical space define a Poisson point process (PPP) If a point process exists, the number of points in any compact cluster $B \subset Rd$ follows a Poisson random variable.

A Poisson point process (PPP) is shown by $\Phi = \{x(i): i = 1, 2,...\} \subset Rd$. Rd is called d-dimensional space while discussing the actual plane. In discrete sets, There is a Poisson distribution and an independent number of points. The $\Lambda = \sum B$ intensity measure In this distribution, the Poisson random variable of density $\lambda(x)$ provides $\lambda(x)dx$. When $\lambda(x)$ remains constant ($\lambda(x) = \lambda$), the PPP is referred to as uniform or homogeneous PPP (HPPP) [25]. Specifically, the expected number of points within a set B is described by an intensity measure that looks like this.

The distribution of N(B) has a Poisson distribution with a mean of $\lambda|B|$ for any compact cluster B, if $|.|$ is the Lebesgue measure of set B.

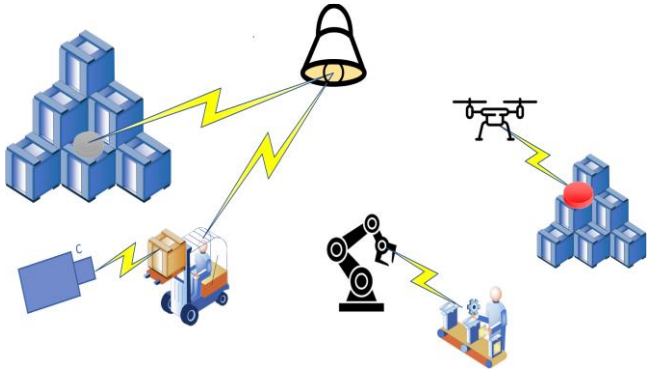

Fig 1: Industrial LiFi network with the AP and IIoT devices

Following the guidelines in [27], the Poisson point process (PPP), represented by Φ with density λ, is used to tessellate the cluster B into a two-dimensional Euclidean space. It is known as the Voronoi tessellation, and it divides the plane into n convex polytopes. Access points (APs) are arranged in the network based on separate PPPs at a density of λp. Furthermore, the Industrial Internet-of-Things (IIoT) devices are classified as D2D transmitting and D2D receiving IIoT, which are implemented independently based on PPPs with densities of λr and λt, respectively. This modelling technique helps create more realistic scenarios and improves the ease of optimisation procedures, such as the research of mobility management. An example of a very dense industrial LiFi network deployment is shown in the supplied figure, which has a variety of IIoT devices.

A. LiFi Channel Model:

During surveying and inspection activities, mobile IoT equipment frequently transmit high-definition video and other data-intensive sensor information in the demanding settings of industrial LiFi deployments. In ultra-dense industrial LiFi networks, mobility management for D2D communication is closely linked to the received optical intensity (ROI). More specifically, measured ROIs are used to determine when to start the process of connecting two IIoT devices. The study only considers line-of-sight (LOS) situations for the LiFi channel model, ignoring the impacts of numerous reflections from objects and human shadowing. The discussion in [28] addresses the validity of this assumption on the insignificance of reflection routes on ROIs. Based on this supposition, the ROI of D2D IIoTs that are received by both the APs and the D2D IIoTs that are sending may be represented as follows

$$\mathrm{ROI}_i(d_{i,u}) = P_i \frac{(m_i+1)A_r}{2\pi d_{i,u}^2} \cos^{m_i}(\varphi_i) T_s g(\psi_i) \cos(\psi_i) \quad (4)$$

where each term represents the direct link (i = k) and D2D link (i = n), respectively. Additionally, di,u denotes the distance from the D2D receiving IIoT to a transmitter point i, Pi is the transmitted power; Ar is the effective area of the receiver; ψi is the angle of incidence with respect to the axis normal to the receiver surface; ϕi is the angle of irradiance with respect to the axis normal to the transmitter surface; ψcon and g(ψi) are the concentrator gain and field-of-view, respectively; and Ts is the filter transmission. Moreover, the Lambertian index, or mi, is described as follows:

$$m_i = -\frac{\ln(2)}{\ln[\cos(\varphi_{1/2})]} \quad (5)$$

The semi angle of the transmitter at half illuminance is represented by υ1/2. Furthermore, the following is a description of the optical concentrator's gain at the receiver:

$$g(\psi) = \begin{cases} \eta^2 / \sin^2(\psi_{\mathrm{con}}), & \text{if } 0 < \psi \le \psi_{\mathrm{con}} \\ 0, & \text{if } \psi_{\mathrm{con}} \le 0 \end{cases} \quad (6)$$

where η is the refractive index.

IV. MOBILITY MODEL

Because it can effectively capture the movement patterns of D2D communication within extremely dense industrial LiFi networks, the random waypoint (RWP) mobility model was used [30]. According to this concept, mobile IIoT devices function inside a specified region, A, and choose their next course of action, or waypoints, evenly throughout A. They then continue to travel at a steady speed in a straight path from their starting place to the newly established waypoint. IIoT devices may optionally include a random halt period before to proceeding to the following waypoint. Three parameters are chosen by the mobile IIoT device at each waypoint: a uniformly distributed random direction on [0, 2π], a transition length that follows a uniform distribution, and a speed that is determined by a uniform distribution. Following the selection of these criteria, the The gadget travels at the designated speed to the next waypoint, which is decided by the direction and transition duration selected. It is impossible to achieve flawless modelling due to the extremely complicated time- and space-varying movement patterns of mobile machines and humans [31][32]. Their extremely scenario- and environment-dependent movement patterns are further complicated by the presence of tangible items. This article makes the assumption that IIoT

device movement adheres to the RWP mobility model, even if it does not concentrate on enhancing movement modelling. Using this model makes it possible to examine how IIoT devices affect LiFi networks and to learn more about building dependable industrial networks. Our framework may be expanded to different mobility models, even though it is centred on the RWP model .We use an endless series of quadruples {(Xk−1,Xk, Vk, Sk)}k∈K, where k represents the kth movement phase, to illustrate the RWP mobility model. The beginning waypoint is denoted by Xk−1, the goal waypoint by Xk, the velocity by Vk, and the pause time at waypoint Xk by Sk inside each period. The next waypoint is determined after a homogeneous PPP Φu(k) with density λu is separately created, beginning from the starting waypoint Xk−1.

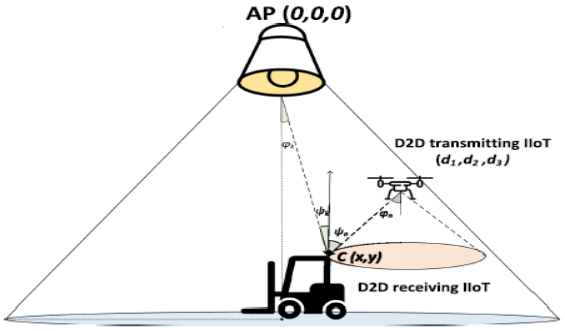

nearest point in Φ*u*(*k*) is selected as the target waypoint. That is

$$\mathbf{X}_k = \arg\min_{\mathbf{x}\in\Phi_u(k)}|\mathrm{x} - \mathbf{X}_{k-1}|. \qquad (7)$$

Consequently, the distance between Xk−1 and Xk is used to compute Lk, which stands for the transition length of the kth movement. This is how the cumulative distribution function (or CDF) of Lk may be expressed:

$$P_{L_k}(L_k \le l) = 1 - \exp(-\lambda_u \pi l^2), \quad l > 0. \qquad (8)$$

The velocity Vk and pause time Sk are independent and identically distributed (i.i.d.) with distributions PV(.) and PS(.), respectively. Moreover, the transition lengths follow a Rayleigh distribution.

V. ANALYTICAL MODEL IN MOVING IIOT DEVICES SCENARIO

In an industrial network, cells are usually located next to one another, and each cell's coverage area is defined by the cells next to it. The received optical intensity (ROI) is the primary criteria used in LiFi networks to shape cell boundaries [30]. The IEEE 802.11bb Task Group on Light Communications' "Manufacturing Cell" specifications are followed in this study's transmitter and receiver placements [19]. These standards take into consideration the scenario when a number of robots function as IIoT devices in a manufacturing setting, with the faces of the devices facing upward. Furthermore, IIoT devices in industrial LiFi networks are presumed to function in a two-dimensional area.IIoT devices are initially dispersed throughout the service area of Access Points (APs) due to the D2D communication mobility pattern, as seen in Fig. 2. IIoT devices are positioned below the APs, which act as an umbrella tier. Thus, every IIoT device is under an AP's coverage. In this case, upon moving inside or outside of the D2D communication coverage region, IIoT devices start the mode selection procedure. A typical AP is situated at the origin, and the position xt(d1, d2, d3) indicates the location of an IIoT device without losing generality. The coverage boundary of IIoT devices broadcasting D2D may be identified by using the ROI measure.

$$C = \{(x,y) \in \mathbb{R}^2 \mid \mathrm{ROI}_k(d_{k,u}) = \mathrm{ROI}_n(d_{n,u})\}. \qquad (9)$$

As a result, as shown in (9), the coverage boundary of the D2D communication range consists of a cluster of equal ROI points. Mobility management parameters for an These points may be utilised to obtain an industrial LiFi network. For a D2D receiving IIoT positioned at coordinates (x, y) ∈ R2 and a height h from the ground, the distances to the AP and the D2D transmitting IIoT are given, respectively, by [35].

$$d_{k,u} = \sqrt{x^2 + y^2 + h^2} \qquad (10)$$

$$d_{n,u} = \sqrt{(x-d_1)^2 + (y-d_2)^2 + (h-d_3)^2}. \qquad (11)$$

In addition,

$$\cos(\varphi_k) = \cos(\psi_k) = \frac{h}{\sqrt{x^2+y^2+h^2}}$$

Because IIoT device faces are directed upward. By substituting (10) and (11) into (9), we obtain

$$W.(x^2 + y^2 + h^2)^{\widehat{m}} - [(x-d_1)^2 + (y-d_2)^2 + (h-d_3)^2] = 0 \qquad (12)$$

where,

$$W=\left(\frac{\mathrm{P_n}(m_n+1)(h-\mathrm{d_3})^{m_n+1}}{\mathrm{P_k}(m_k+1)h^{m_k+1}}\right)^{\frac{2}{m_n+3}},\ \widehat{m}=\frac{m_k+3}{m_n+3}.$$

It is now assumed that all of the transmitters in the system have the same Lambertian index. As a result, the Lambertian index of the AP and the D2D sending IIoT is identical (mk = mn), where _m = 1. Thus, the geometry of a circle is defined by equation (12). The radius, Rc, and the corresponding centre, xc = (xc, yc), are computed as

$$\mathrm{x_c}=\left(\frac{d_1}{1-W},\frac{d_2}{1-W}\right) \quad (13)$$

$$R_c=\sqrt{\frac{W({d_1}^2+{d_2}^2)}{(1-W)^2}+\frac{Wh^2-(h-d_3)^2}{(1-W)}}. \quad (14)$$

The suggested coverage boundary of D2D communication and stochastic geometry may be used to create an analytical model for mode selection in moving D2D situations. One D2D receiving IIoT device and several D2D transmitting IIoT devices dispersed in accordance with the properties of a Poisson point process (PPP) can simplify the scenario. It is clear from equation (14) that the D2D communication range depends on the location of the IIoT device that is broadcasting D2D. On the other hand, the mode of the D2D receiving IIoT is determined by the relative distance between IIoTs. Subscript "c" is used to represent the D2D communication range centre transition length for clarity, while superscript "_" is used to represent the relative movement transition length. Fig. 3(a) illustrates how the D2D sending IIoT is located at waypoint Xn−1 and proceeds, in the next step, to waypoint Xn, with the origin serving as the location of the AP. It is possible to calculate the transition length of the centre of the coverage border by taking use of the parallel relationship between the lines Xn−1Xn and Cn−1Cn.

$$L_c=L\times\sqrt{\frac{(\frac{d_1}{1-W})^2+(\frac{d_2}{1-W})^2+h^2}{{d_1}^2+{d_2}^2+{d_3}^2}}.$$

The D2D transmitting IIoT might be thought of as travelling in the direction of the reference point, or the receiving IIoT, if the D2D receiving IIoT is assumed to be the reference point. Consequently, the relative

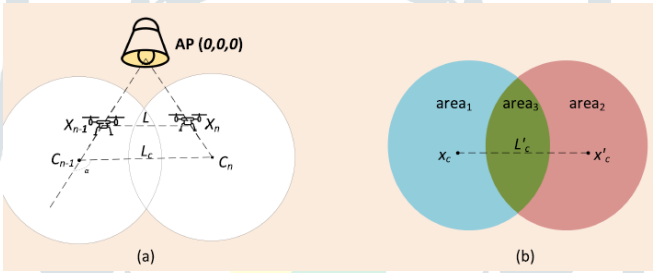

Fig. 3. (a) Changing of D2D communication range. (b) Relative movement analytical framework.

The movement scenario preserves realistic aspects while streamlining the analysis of intricate multiple item movements into a single object movement. The coverage boundary of the D2D transmitter IIoT may be seen both before and after relative movement, as shown in Fig. 3(b). Based on the relative movement of the D2D transmitter IIoT, three unique situations emerge, assuming that the D2D receiver IIoT stays fixed:

- The D2D receiving IIoT will switch from D2D mode to direct mode if it is located in region 1 (the blue area). The reason for this shift is that the IIoT that is sending D2D has moved from area 1 to area 2 (the red region).
- On the other hand, the D2D receiving IIoT will change from direct to D2D mode of communication if it is situated in area 2. This switchtranspires when the IIoT that is broadcasting D2D travels from area 1 to area 2.
- The D2D receiving IIoT will continue to communicate in the same manner if it is positioned in region 3 (the green area).

VI. D2D MOBILITY ANALYSES FOR RESILIENT INDUSTRIAL LIFI NETWORK:

A.Mode Transition Rate

The integration of D2D communication into wireless communication, together with the use of next-generation industrial LiFi systems, will inevitably lead to network densification. Higher transition rates are caused by the smaller and denser cell deployment that results from this densification. Mode transition rate is closely correlated with network signalling cost. The RWP mobility model allows for the division of the IIoT devices' movement trace into an endless number of segments. As a result, the estimated number of D2D mode transitions, E[N], during a single movement period divided by the expected duration of time, E[T], yields the D2D mode transition rate, H.

$$H = \frac{E[N]}{E[T]}. \qquad (15)$$

Considering *n*th movement, the expected number of D2D mode transition is given by

$$E[N] = \lambda_t |\mathcal{A}| E_t[N] \qquad (16)$$

where λt, |A|, and Et[N] stand for the estimated D2D mode transition number for the typical transmitting IIoT, the whole probability space, and the D2D transmitter IIoT density, respectively. According to the suggested model in Fig. 3(b), the likelihood that the IIoT situated in area1 and area2 would conduct a D2Dmode transition during the kth movement period is represented as

$\frac{S_{\text{area}_1} + S_{\text{area}_2}}{|\mathcal{A}|}$

or an average IIoT that transmits D2D. For the IIoT that is transmitting D2D data, the anticipated D2D mode transition number is obtained.

$$E_t[N] = \int\int \frac{S_{\text{area}_1} + S_{\text{area}_2}}{|\mathcal{A}|} f_{L_c'}(l) f_{R_c}(r) dl dr \qquad (17)$$

Essential parameters are the probability density function (PDF) of the D2D coverage radius (fR_c(r)) and the circle centre relative movement transition length (fL_c(l). The total area S may be calculated as the sum of S_area1 and S_area2, as shown in Fig. 3. It is notable that the expression in (14) and the values of W are much less than 1, indicating that the D2D communication range is nearly constant before and after the movement. This suggests that the radius of the circle stays almost constant. As a result, two circles of the same radius (R_c = R_c) fit the analytical framework nicely. This gives the phrase for S.

$$S = \begin{cases} 2\pi R_c^2 - 4R_c^2 \arccos\frac{L_c'}{2R_c} + 2L_c'\sqrt{R_c^2 - \frac{L_c'^2}{4}}, & L_c' < 2R_c \\ 2\pi R_c^2, & L_c' \geq 2R_c \end{cases} \qquad (18)$$

If we regard *S* as a function of *L_ C 2Rc* , we can approximate it by using the Taylor series expansion and get the expected D2D mode transition number for a typical transmitting IIoT as

$$\begin{aligned} E_t[N] &= \int\int \frac{4\tilde{}lr}{|\mathcal{A}|} f_{L_c'}(l) f_{R_c}(r) dl dr \\ &= \frac{4}{|\mathcal{A}|} E[L_c'] E[R_c]. \end{aligned} \qquad (19)$$

As a result, the D2D mode transition rate can be expressed as closed-form as

$$\begin{aligned} H &= 4\lambda_t v E[R_c] \sqrt{\frac{\left(\frac{d_1}{1-W}\right)^2 + \left(\frac{d_2}{1-W}\right)^2 + h^2}{{d_1}^2 + {d_2}^2 + {d_3}^2}} \\ &= 4\lambda_t v \sqrt{\frac{W E[X_{p2t}]^2}{(1-W)^2} + \frac{Wh^2 - (h-d_3)^2}{(1-W)}} \\ &\quad \times \sqrt{\frac{\left(\frac{d_1}{1-W}\right)^2 + \left(\frac{d_2}{1-W}\right)^2 + h^2}{{d_1}^2 + {d_2}^2 + {d_3}^2}} \\ &= 4\lambda_t v \sqrt{\frac{W}{4\lambda_p (1-W)^2} + \frac{Wh^2 - (h-d_3)^2}{(1-W)}} \\ &\quad \times \sqrt{\frac{\left(\frac{d_1}{1-W}\right)^2 + \left(\frac{d_2}{1-W}\right)^2 + h^2}{{d_1}^2 + {d_2}^2 + {d_3}^2}} \end{aligned} \qquad (20)$$

where the estimated distance, based on stochastic geometry, between the AP and the D2D sending IIoT is provided.

$$E[X_{p2t}] = \frac{1}{2\sqrt{\lambda_p}}$$

B. D2D Residence Time:

Residence time is a term used to characterise the predicted IIoT dwell time interval in a D2D communication range [40]. The predicted D2D mode residence time may be easily obtained with defined mode change regions. Given the percentage of covered locations, the likelihood of receiving IIoT—which uses a D2D communication mode—is important.

$$\frac{\pi R_c^2}{|\mathcal{A}|}.$$

Also, the probability that the receiving IIoT changes its communication mode from D2D mode to direct mode after the relative movement is

$$\frac{S_{\text{area1}}}{|\mathcal{A}|}$$

Thus, the probability of $Lt < l$ can be obtained as

$$P(L_t \le l) = \frac{S_{\text{area1}}}{\pi R_c^2} = 1 - \frac{2}{\pi}\arccos\frac{l}{2R_c} + \frac{l}{\pi R_c^2}\sqrt{R_c^2 - \frac{l^2}{4}}. \tag{21}$$

In addition, the PDF of the trajectory length Lt is derived as

$$f_{L_t} = \frac{1}{\pi R_c}\left(\frac{4\pi R_c^3 - l^2}{4\pi R_c^3\sqrt{1-(l/2R_c)^2}} + \sqrt{1-(l/2R_c)^2}\right). \tag{22}$$

In the final stage, the D2D mode residence time and predicted trajectory length inside a D2D communication range are provided, respectively, by

$$E[L] = \int\int_0^{2r} l f_{L_t(l)} f_{R_c(r)} dl dr$$

$$= \frac{\pi}{2}\sqrt{\frac{W}{4\lambda_p(1-W)^2} + \frac{Wh^2 - (h-d_3)^2}{(1-W)}} \tag{23}$$

$$T = \frac{E[L]}{E[V]} = \frac{\pi}{2v}\sqrt{\frac{W}{4\lambda_p(1-W)^2} + \frac{Wh^2 - (h-d_3)^2}{(1-W)}}. \tag{24}$$

VII. RESULTS

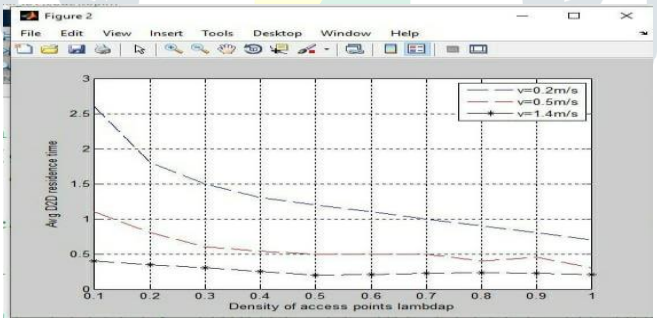

FIGER4:AverageD2Dmodetransitionratebyanalysesandsimulation.

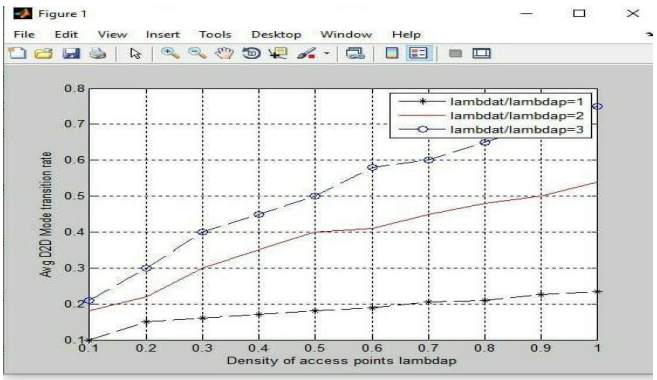

Fig.5.:AverageD2Dresidencetimebyanalysesandsimulation.

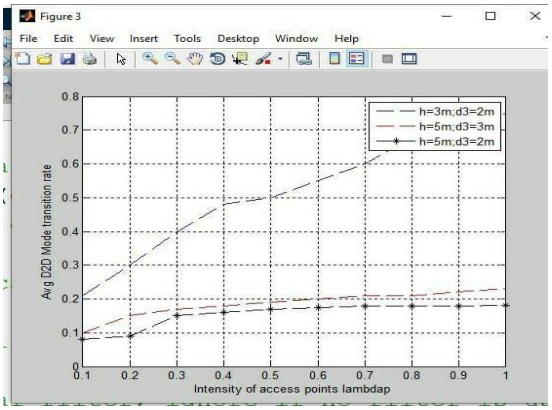

Fig. 6. Average D2D mode transition rate for different heights from the ground

CONCLUSION

This study analyses the important performance indicators for the mode shift from the AP to the D2D transmitting IIoT in ultra-dense industrial LiFi networks for D2D communication. The analytical model for the coverage regions of D2D communication is developed, based on semi angle at half illuminance. Furthermore, as functions of the system parameters, closed-form formulas for the D2D mode transition rate and the D2D dwell time are given. As can be seen from the closed-form formulas, velocity, IIoT density, and AP density are important factors in D2Dmobility management in ultradense industrial LiFi networks. Furthermore, the provided analytical formulations are validated by simulation results. The findings have significance for the design, implementation, and mode selection of industrial LiFi.

Future scope

In D2D communication, the most important question is how to provide effective security. With regard to risks, this addition has provided an evaluation of security-related concerns and suggested areas for improvement. Nonetheless, our investigation has led us to the conclusion that there are no international policy guidelines governing the safe interplay of user equipment. Since there are differences in the authentication systems utilised, achieving interoperability is challenging.

REFERENCES

F. Jejdling *et al.*, "Ericssonmobility report,"Ericsson, Stockholm, Sweden,Tech. Rep., Nov. 2020.

Cisco, "Cisco service provider Wi-Fi: A platform for business innovationand revenue generation," CISCO White Paper, ID:1458684054151755, Nov. 2012.

3GPP, "LTE device to device proximity services; user equipment (UE)radio transmission and reception, 3GPP 36. 877," Version 0.0.4 Release 12, 2014.

Z. Ghassemlooy, W. Popoola, and S. Rajbhandari, *Optical Wireless Communications:*System and Channel Modelling With Matlab. Boca Raton, FL, USA: CRC Press, 2019.

3GPP, "Requirements for evolved utra (e-utra) and evolved utran (eutran),"Version 8.0.0 Release 8, 2009.

H. Zhang,W. Ding, J. Song, and Z.Han, "Ahierarchical game approach forvisible light communication and D2D heterogeneous network," in *Proc.* IEEE Glob. Commun. Conf., 2016, pp. 1–6.

H. Zhang, W. Ding, F. Yang, J. Song, and Z. Han, "Resource allocationin heterogeneous network with visible light communication and D2D: A hierarchical game approach," *IEEE Trans. Commun.*, vol. 67, no. 11, pp. 7616–7628, Nov. 2019.

M. Najla, P. Mach, Z. Becvar, P. Chvojka, and S. Zvanovec, "Efficientexploitation of radio frequency and visible light communication bands for D2D inmobile networks," *IEEE Access*, vol. 7, pp. 168922–168933, 2019.

M. Najla, P. Mach, and Z. Becvar, "Deep learning for selection betweenRF and VLC bands in device-to-device communication," *IEEE Wireless Commun. Lett.*, vol. 9, no. 10, pp. 1763–1767, Oct. 2020.

P. Mach, Z. Becvar, M. Najla, and S. Zvanovec, "Combination of visiblelight and radio frequency bands for device-to-device communication," inProc. IEEE 28th Annu. Int. Symp. Pers., Indoor, Mobile Radio Commun.,2017, pp. 1–7.

Z. Becvar, M. Najla, and P. Mach, "Selection between radio frequencyand visible light communication bands for D2D," in *Proc. IEEE 87th Veh. Technol. Conf.*, 2018, pp. 1–7.

Z. Becvar, R.-G. Cheng, M. Charvat, and P.Mach, "Mobility managementfor D2D communication combining radio frequency and visible lightcommunications bands," *Wireless Netw.*, vol. 26, no. 7, pp. 5473–5484,2020.

N. Raveendran, H. Zhang, D. Niyato, F. Yang, J. Song, and Z. Han, "VLCand D2D heterogeneous network optimization: A reinforcement learning approach based on equilibrium problems with equilibrium constraints,"*IEEE Trans. Wireless Commun.*, vol. 18, no. 2, pp. 1115–1127, Feb. 2019.

S. V. Tiwari, A. Sewaiwar, and Y.-H. Chung, "Optical repeater assistedvisible light device-to-device communications," *Int. J. Electron. Commun.Eng.*, vol. 10, no. 2, pp. 206–209, 2016.

Y. Liu, Z. Huang,W. Li, and Y. Ji, "Game theory-based mode cooperativeselection mechanism for device-to-device visible light communication," *Opt. Eng.*, vol. 55, no. 3, 2016, Art. no. 030501.

Z. N. Chaleshtori, S. Zvanovec, Z. Ghassemlooy, O. Haddad, and M.-A.Khalighi, "Impact of receiver orientation on oled-based visible-light D2D communications," in Proc. 17th Int. Symp. Wireless Commun. Syst., 2021,pp. 1–6.

[17] Z. N. Chaleshtori, S. Zvanovec, Z. Ghassemlooy, and M.-A. Khalighi,"Visible light communication with oleds for D2D communications consideringuser movement and receiver orientations," *Appl. Opt.*, vol. 61,no. 3, pp. 676–682, 2022.

[18] P. Kumar *et al.*, "Challenges and applications of Li-Fi in D2D communication,"in Proc. Int. Conf. Commun., Control Inf. Sci., 2021, vol. 1, pp. 1–6.

[19] M. Uysal, F. Miramirkhani, T. Baykas, and K. Qaraqe, "IEEE 802.11-18/1582r0 BB reference channel models for indoor environments," Tech.